Journal of Associated Medical Sciences 2026; 59(1): 62-72

JAMS
Journal of Associated Medical Sciences

Scopus Indexed & Thai-Journal Citation Index Centre (TCI)

Journal of Associated Medical Sciences

Journal homepage: https://www.tci-thaijo.org/index.php/bulletinAMS/index

Gamma ray interaction of germanoborate glasses for radiation shielding applications

Natthakridta Chanthima[1,2], Supakit Yonphan[1,2], Chalermpon Mutuwong[1,2], Wuttichai Chaiphaksa[1,2*], Jakrapong Kaewkhao[1,2]

[1]Physics program, Faculty of Science and Technology, Nakhon Pathom Rajabhat University, Nakhon Pathom Province, Thailand.
[2]Center of Excellence in Glass Technology and Materials Science (CEGM), Nakhon Pathom Rajabhat University, Nakhon Pathom Province, Thailand.

ARTICLE INFO

Article history:
Received 28 June 2025
Accepted as revised 29 August 2025
Available online 16 September 2025

Keywords:
Glass, gadolinium, radiation shielding, WinXCom.

ABSTRACT

Background: Ionizing radiation is essential in medical imaging and therapy, but it also poses health risks to medical staff and patients. Traditional shielding materials like lead are effective but toxic, while concrete lacks transparency. Therefore, glass systems incorporating high-Z oxides offer a promising alternative by combining optical clarity with enhanced radiation shielding performance.

Objectives: This study aims to develop and investigate germanoborate glasses doped with Gd_2O_3, with a particular focus on their photon attenuation properties. The findings are intended to development of transparent, lead-free radiation shielding materials suitable for medical and industrial applications.

Materials and methods: The Gd_2O_3 added germanoborate glasses in the system (60-x)B_2O_3-GeO_2-x Gd_2O_3 (with x=10, 20, 30 and 40 mol%) were synthesized via melting at 1400 °C followed by melt quenching method. The densities were measured by Archimedes' method. The mass attenuation coefficients (μ_m), the effective atomic number (Z_{eff}), the effective electron density (N_{eff}), and half-value layers (HVL) were computed using the WinXCom program (NIST XCOM Database) to assess shielding properties. PHITS Monte Carlo simulations were employed to calculate the effective dose rate.

Results: The addition of Gd_2O_3 increased the glass density from 3.7546 gm/cm^3 to 5.4604 gm/cm^3. Replacing B_2O_3 with Gd_2O_3 enhanced the mass attenuation coefficients (μ_m), effective atomic number (Zeff) and effective electron density (Neff). HVL values decreased, Pb equivalent values increased, and the effective dose was reduced.

Conclusion: The incorporation of Gd_2O_3 into germanoborate glasses significantly enhances their gamma-ray attenuation capabilities, confirming their effectiveness as lead-free shielding materials. The developed glasses exhibit optimized radiation protection properties, highlighting their potential for transparent shielding applications in medical, industrial, and nuclear fields. and infliximab exert protective effects on liver function in acetic acid induced UC model. These findings suggest potential benefits of these therapies in mitigating liver damage associated with UC, highlighting the importance of considering liver health in UC management.

*** Corresponding contributor.**
Author's Address: *Physics program, Faculty of Science and Technology, Nakhon Pathom Rajabhat University, Nakhon Pathom Province, Thailand.*
E-mail address: wuttichai@webmail.npru.ac.th
doi: 10.12982/JAMS.2026.009
E-ISSN: 2539-6056

Introduction

Ionizing radiation is essential in modern diagnostic imaging and radiation therapy. However, its use involves potential risks of radiation dose received by both

healthcare professionals and patients. Accordingly, the development and implementation of effective radiation protection methods are essential to minimize exposure and ensure safety in environments where radiation is routinely used.[1] The effectiveness of a shielding material is largely determined by its density and atomic composition. Materials with high atomic number (Z) and high density present more electrons per unit volume, leading to a higher probability of photon interactions. In the energy range used for medical imaging and therapy, the dominant photon interactions are the photoelectric effect and Compton scattering High-Z, high-density materials strongly enhance photoelectric absorption, while Compton scattering depends mainly on total electron density.[2] Lead (Pb) is a commonly used shielding material due to its high density, low cost, and ease of fabrication. Nevertheless, the toxic nature of lead poses serious environmental and health concerns, prompting the need for alternative, ecofriendly shielding materials.[3] As a result, lead free shielding materials have gained considerable attention. Concrete is another traditional bulk shielding material. It is inexpensive, easily cast into walls or blocks, and has good mechanical strength. Ordinary concrete is effective for gamma shielding partly because it can incorporate heavy aggregates to raise its density. However, its opacity limits its use in certain medical applications that require visibility.

Glass materials have emerged as a promising alternative due to their transparency, chemical versatility, and ability to be tailored for specific radiation shielding applications. By incorporating heavy metal oxides into the glass matrix, their density and photon attenuation capabilities can be significantly enhanced. Thus, by incorporating heavy metal oxides into transparent glasses, it is possible to create shields that approach the performance of lead while still allowing light to pass through.[4] Borate glasses are valued as host materials because they form stable, dense networks with desirable thermal and mechanical performance. They exhibit high thermal stability and excellent glass forming ability. In practice, borate glasses can incorporate modifiers to further increase density and hardness without crystallization. These features make borate matrices resistant to cracking and thermal shock, and well suited for optical transparency.[5]

Adding GeO_2 is known to improve network connectivity and optical transmission in borate glasses. GeO_2 is a relatively dense glass former (ρ = 4.25 g/cm^3) characterized by a high refractive index and a broad infrared transmission window. GeO_2 doped glasses generally exhibit lower phonon energies (800-975 cm^1) compared to borate-based glasses. As a result, the incorporation of GeO_2 into a glass matrix effectively reduces the overall host phonon energy. As a result, germanoborate glasses can exhibit higher refractive index and broader optical transparency, as well as increased glass transition temperature, all of which strengthen the network.[4] For radiation shielding, Gadolinium oxide is an especially attractive dopant for gamma shielding. Gd has a high atomic number (Z=64) and density (7.895 g/cm^3), which contribute to enhanced photoelectric absorption and Compton scattering interactions with gamma photons. Importantly, Gd_2O_3 does not induce radiation related color centers in glass. In fact, several studies have reported that Gd_2O_3 acts as a heavy metal modifier, increasing the glass density and enhancing gamma-ray attenuation while maintaining optical transparency.[6] Moreover, PHITS Monte Carlo simulation was employed to simulate radiation transport and assess absorbed dose distributions in the context of modern diagnostic imaging and radiation therapy.

In this work, the Gd_2O_3 added germanoborate glasses were fabricated using a melt quenching technique. The obtained samples were analyzed for their density, structure, and radiation properties. The photon attenuation parameters were determined using WinXCom software, which extracts data from the NIST database. WinXCom is an accepted reference for X-ray and gamma ray interaction coefficients and has been widely used in glass shielding studies.[7]

Materials and methods

Theoretical background

The gamma ray attenuation in materials follows the exponential Beer-Lambert law:

$$I = I_0 e^{-\mu x}, \quad (1)$$

where I and I_0 are the transmitted and incident intensities, μ is the linear attenuation coefficient (cm^{-1}), x and is the thickness (cm).The mass attenuation coefficient (μ_m) is calculated by normalizing μ to the material's density, and provides a density independent measure of attenuation:

$$\mu_m = \sum_i w_i \left(\frac{\mu}{\rho}\right)_i, \quad (2)$$

When w_i is the fractional weight, and μ_m is the mass attenuation coefficient of each element. Theoretical calculations can be performed using the WinXCom software, which provides tabulated photoncross sections based on composition and energy.[8]

The total atomic cross section, (σ_a), can be evaluated from the values of the total mass attenuation coefficients by the following

$$\sigma_a = \frac{\mu}{N_A \sum_i \frac{w_i}{A_i}}, \quad (4)$$

Similarly, the total electronic cross section, (σ_e), is given by the following formula

$$\sigma_e = \frac{1}{N_A}\sum_i \left(\sum_i \frac{f_i A_i}{Z_i} \right) w_i \quad ,(5)$$

where f_i and Z_i are respectively the fractional abundance and the atomic number of each element. For compound materials, the effective atomic number (Z_{eff}), is defined as the ratio between the total atomic effective cross section and the total electronic effective cross section.

$$Z_{eff} = \frac{\sigma_a}{\sigma_{el}} \quad ,(6)$$

The effective electron density (N_{eff}) defines the electrons number per unit mass, which is related to the Z_{eff}, is formulated as follows.[9]

$$N_{eff} = N_A \frac{Z_{eff}}{\sum_i \frac{w_i}{A_i}} \quad ,(7)$$

The half value layer (HVL), defined as the thickness of material required to reduce the intensity by half, it is given by:

$$HVL = \frac{0.693}{\mu} \quad ,(8)$$

where μ is the linear attenuation coefficient. HVL is a practical parameter for assessing and comparing the shielding effectiveness of different materials.[10]

Lead equivalent thickness refers to the thickness of lead that would provide an identical shielding performance against radiation as the material under investigation, under the same specified conditions. The degree of shielding can be evaluated through the material's transmission factor. For photons of a particular energy passing through a certain thickness of material or lead, the relationship between the linear attenuation coefficient (LAC) and thickness allows for the estimation of the equivalent lead thickness.[11] This can be expressed as:

$$d_{pb} = \frac{\mu_{material}}{\mu_{pb}} \times d_{material} \quad ,(9)$$

where μ_{pb} denotes the LAC of lead, d_{pb} represents the calculated lead equivalent thickness, $\mu_{material}$ is the LAC of the material, and $d_{material}$ is the thickness of that material.

Sample preparations

The Gd_2O_3 added germanoborate glasses to radiation shielding were prepared by melt quenching technique in compositions of (60-x)B_2O_3-GeO_2-xGd_2O_3 (with x=10, 20, 30 and 40 mol%). Each batch was melted in alumina crucibles by an electrical furnace for about 3 hrs, at 1400 °C and poured into the graphite mold at room temperature and annealed at 500 °C for 3 hrs. All glass samples were cut and polished into a size about 1 cm × 1.5 cm x 0.3 cm for more investigations.

WinXCom program

WinXCom is a software implementation of the NIST XCOM photon cross-section database. It provides theoretical mass attenuation coefficients and partial interaction cross sections (photoelectric absorption, Compton scattering, pair production) for any element, compound or mixture over a wide photon energy range (approximately 1 keV to 100 GeV). Users simply specify the material's composition (by chemical formula or elemental mix) and the energy range of interest, and WinXCom computes the attenuation data. The output includes not only the mass attenuation coefficients but also allows derivation of composite parameters such as the effective atomic number and effective electron density, which are standard metrics for quantifying gamma-ray shielding effectiveness. The main advantages of WinXCom are its speed and versatility: it can rapidly generate attenuation data for a vast range of materials and energies, greatly aiding the design and optimization of novel radiation shields. For these reasons it has become an essential tool in shielding research.[12]

PHITS Monte Carlo simulation

To investigate the absorbed radiation dose, the adult male mesh-type reference computational phantom (MRCP-AM) was implemented in PHITS. The MRCP-AM dataset comprises MRCP-AM.node (nodal data), MRCP-AM.ele (element connectivity), MRCP-AM.cell (geometric configuration, spatial location, and density information), and MRCP-AM.material (material composition), as illustrated in Figure 1. The primary objective was to evaluate the absorbed and effective dose rates within the MRCP-AM phantom, both prior to and following the inclusion of shielding glass, using Monte Carlo simulation techniques. The phantom model was imported into PHITS via the [Surface], [Cell], and [Materials] sections to accurately define the anatomical structure of the entire human body.[13] The irradiation source and anterior-posterior (AP) geometry was defined within the [Source] section, with the source placed at coordinates (0, 0, -60). The shielding glass was defined using the [Surface], [Cell], and [Materials] sections, with dimensions of 60.0 cm × 1.0 cm × 200.0 cm and located at (0, 0, -40). Organ-specific absorbed dose distributions were calculated using the [T-Deposit] section with a "reg" mesh, while effective dose rates, based on ICRP Publication 103 recommendations for AP irradiation geometry,[14] were determined using the [T-Track] section with an "xyz" mesh and the "-202" weighting factor in the [Multiplier] section.[15] A total of 100 million primary photons were simulated to ensure sufficient statistical accuracy.

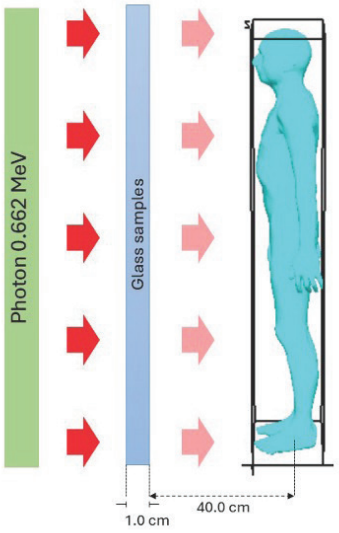

Figure 1. *The MRCP-AM models from PHITS.*[16]

Result and discussions

Physical properties

The physical properties of the Gd_2O_3 added germanoborate glass system with the composition (60-x) B_2O_3-GeO_2-xGd_2O_3 (where x=10, 20, 30, and 40 mol%) were systematically investigated were shown in Figure 2. It was observed that the glass density increased from 3.7546 gm/cm^3 (Gd10) to 5.4604 g/cm^3 (Gd40) as the Gd_2O_3 content increased. This trend is primarily due to the replacement of B_2O_3, a low-density component, with Gd_2O_3 which contains Gd atoms of significantly higher atomic mass (157.25 gm/mol) compared to B (10.81 gm/mol), thereby increasing the overall density of the glass network. Meanwhile, the molar volume increased from 30.0711 cm^3/mol (Gd10) to 37.3287 cm^3/mol (Gd30), reflecting the network expansion due to the formation of non-bridging oxygen (NBO) sites induced by Gd_2O_3. However, a slight decrease in molar volume was observed at 36.7679 cm^3/mol for Gd40, possibly indicating network compaction. This behavior suggests that at high concentrations, Gd^{3+} ions acting as network modifiers with a relatively large ionic radius may disrupt the open structure typically promoted by NBO formation and instead lead to a denser packing.[17,18] These findings demonstrate the structural impact of Gd_2O_3 substitution on the glass network connectivity and packing in Gd_2O_3 added germanoborate glasses.

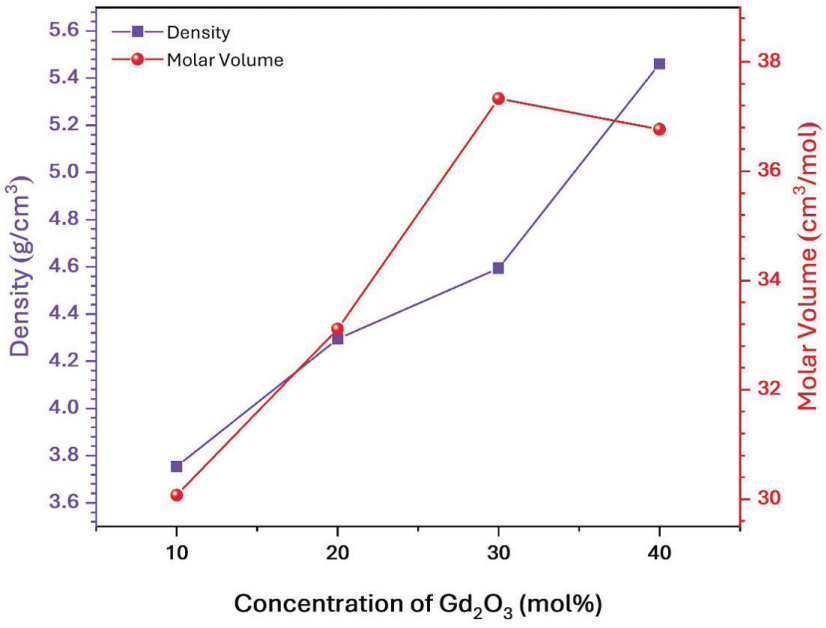

Figure 2. *The density and molar volume of Gd_2O_3 added germanoborate glasses.*

Radiations shielding properties

Figure 3. illustrates the dominant photon interaction mechanisms in germanoborate glass added with 40 mol% Gd_2O_3 over the photon energy range of 0.015-15 MeV. The interactions are categorized into three primary sub processes the photoelectric effect, Compton scattering, and pair production. In the low energy region (below 0.1 MeV), the photoelectric effect is the predominant attenuation mechanism. This is consistent with the increased probability of photon absorption in high atomic number (Z) materials such as gadolinium (Z=64). Notably, a distinct absorption edge, or K-edge, appears near the binding energy of the K-shell electrons of Gd, reflecting a sharp increase in photon attenuation efficiency in this energy region. As photon energy increases into the intermediate range (0.1-1 MeV), Compton scattering becomes the principal interaction, characterized by the elastic scattering of photons. This process is closely related to the materials electron density and plays a critical role in applications requiring intermediate energy radiation shielding, particularly in medical diagnostics and industrial radiography. At higher photon energies (>1.02 MeV), pair production becomes increasingly significant. In this process, a high energy photon is converted into an electron-positron pair when interacting near the nucleus. The rising attenuation coefficient in this region indicates the material's capability to manage high energy photons, which is essential for shielding applications involving linear accelerators and other high energy radiation sources. Overall, the total attenuation curve represents the cumulative contribution of all interaction mechanisms, exhibiting distinct variations as a function of photon energy. The addition of Gd_2O_3 significantly improves photon attenuation efficiency across all energy regions, particularly at lower energies due to the strong influence of the photoelectric effect and the prominent K-edge of Gd.

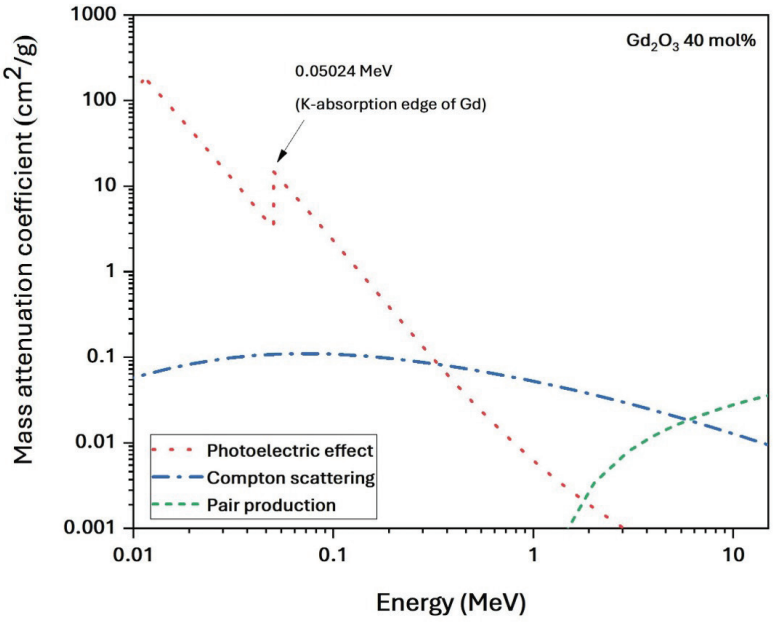

Figure 3. *The partial interaction of Gd_2O_3 added germanoborate glasses.*

The mass attenuation coefficient (μ_m) of germanoborate glasses with the composition (60-x) B_2O_3-GeO_2-xGd_2O_3 (where x=10, 20, 30, 40 mol%) was evaluated across a photon energy range of 0.015 to 15 MeV using the WinXCom software were present in Figure 4. The results revealed that μ_m decreases with increasing photon energy, consistent with the dominant interaction mechanisms governing photon attenuation namely, the photoelectric effect, Compton scattering, and pair production. At low photon energies (<0.2 MeV), the photoelectric effect is the dominant interaction, resulting in a high μ_m value that rapidly decreases as energy increases. A pronounced peak in μ_m was observed around 0.05024 MeV, corresponding to the K-absorption edge of gadolinium (Gd), where photon energy is sufficient to eject K-shell electrons from Gd atoms, significantly enhancing attenuation. Following this sharp rise, μ_m declines steadily in the intermediate energy range (0.2-1 MeV), where Compton scattering becomes the predominant interaction.

In the high energy region (>1.02 MeV), pair production becomes the leading mechanism, characterized by the conversion of high energy photons into electron positron pairs, altering the attenuation behavior based on interaction probability. Comparative analysis of the glasses indicated that increasing the Gd_2O_3 content leads to higher μ_m values, especially in the low energy region. This enhancement is attributed to the high atomic number (Z=64) and density of Gd, which significantly increases the probability of the photoelectric effect. However, at higher photon energies, the influence of Gd content on μ_m becomes less significant, as the

dominant interactions. Compton scattering and pair production are less sensitive to atomic number.[19] These findings demonstrate that germanoborate glasses added with higher concentrations of Gd_2O_3 are particularly effective in attenuating gamma radiation, making them promising candidates for radiation shielding applications.

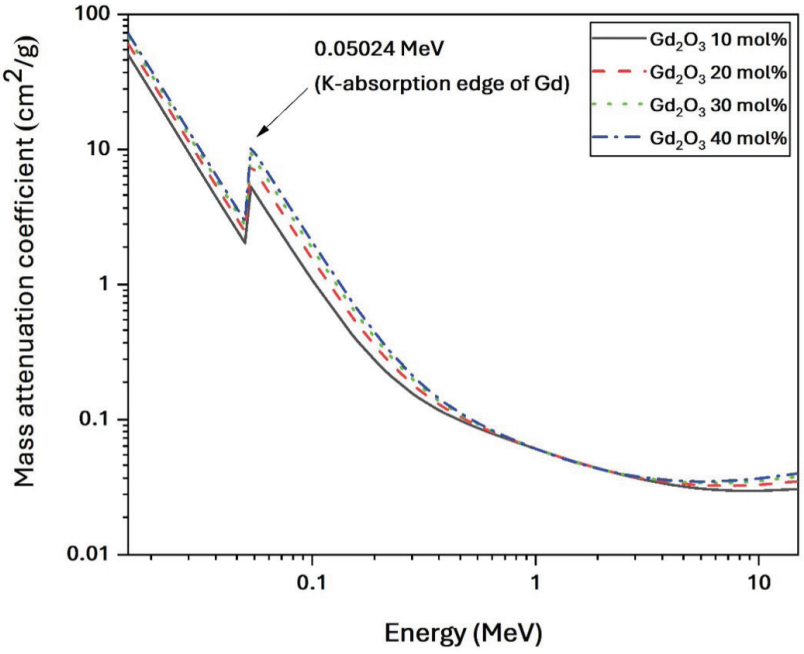

Figure 4. *The mass attenuation coefficient of Gd_2O_3 added germanoborate glasses.*

Figure 5. illustrates the variation of the effective atomic number (Zeff) of germanoborate glasses with different Gd_2O_3 contents (10-40 mol%) over a photon energy range of 0.015 to 15 MeV. The Zeff values show a strong dependence on photon energy, governed by the underlying photon interaction mechanisms. At lower energies (below 0.1 MeV), Zeff exhibits relatively high values, particularly for glasses with higher Gd_2O_3 content. This enhancement is due to the photoelectric effect, which strongly favors high atomic number constituents such as gadolinium (Z = 64). As a result, the substitution of B_2O_3 with Gd_2O_3 significantly elevates the effective atomic number in this region. A distinctive peak in Zeff is observed around 0.05024 MeV, which corresponds to the K-absorption edge of gadolinium. At this energy, photons possess sufficient energy to eject K-shell electrons, leading to a sharp rise in the interaction cross section and a corresponding sudden rise in Zeff. This localized increase reinforces the role of Gd in enhancing photoelectric absorption near its characteristic absorption edge. Beyond the absorption edge, Zeff values gradually decline with increasing photon energy, reaching a minimum in the intermediate range (approximately 0.2-2 MeV). This behavior corresponds to the dominance of Compton scattering, which is less sensitive to the atomic number and more dependent on the electron density of the material. In this range, the Zeff values for different Gd_2O_3 contents tend to converge, reflecting the diminished influence of high Z elements. At higher photon energies (>1.02 MeV), Zeff shows a slight upward trend, attributed to the onset of pair production, a process that becomes increasingly significant at high energies and is again influenced by the atomic number of the absorbing material. Overall, the variation of Zeff across the energy spectrum closely aligns with the trends observed in the μ_m, particularly in the photoelectric region. The incorporation of Gd_2O_3 not only elevates Zeff at low energies but also enhances the glass's photon interaction potential across a broad energy range, confirming its suitability for applications requiring efficient gamma ray shielding.

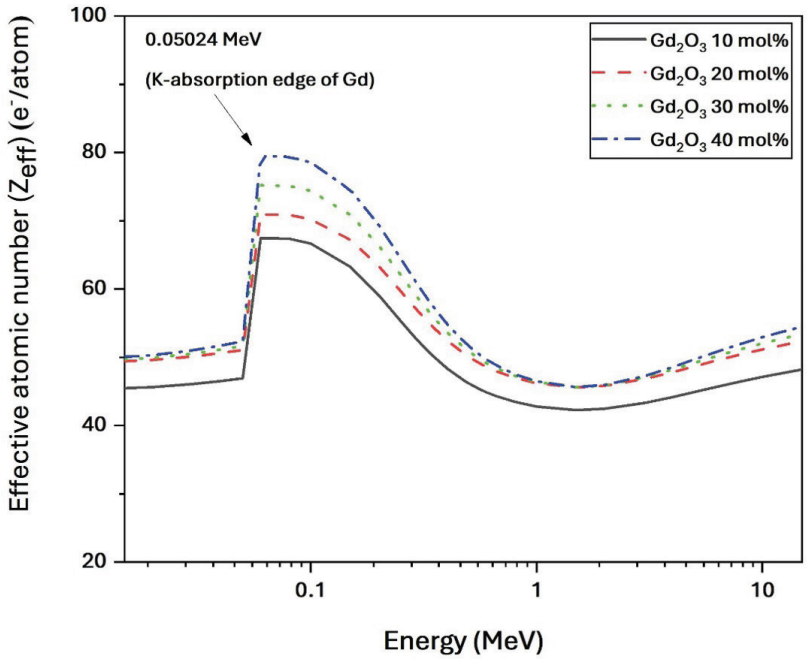

Figure 5. *The effective atomic number of Gd_2O_3 added germanoborate glasses.*

The variation of effective electron density (Neff) in Gd_2O_3 added germanoborate glasses, as shown in Figure 6., generally follows a trend similar to that of Um and Zeff, reflecting the dominant photon interaction mechanisms across energy ranges. However, it is noteworthy that (<0.05 MeV) the Neff values show inversion from the 10 mol% and 40 mol% Gd_2O_3 samples, with the 10 mol% composition exhibiting the highest Neff values. This behavior may result from the complex interplay between the increase in atomic number and the corresponding mass increase, which affects the electron density per unit mass. Furthermore, a pronounced peak is evident near the K-absorption edge of Gd, attributed to the photoelectric effect. Overall, Neff values decrease gradually with increasing photon energy, ranging from higher values at low energies to lower values at high energies, consistent with the energy dependent nature of radiation-matter interactions.[19]

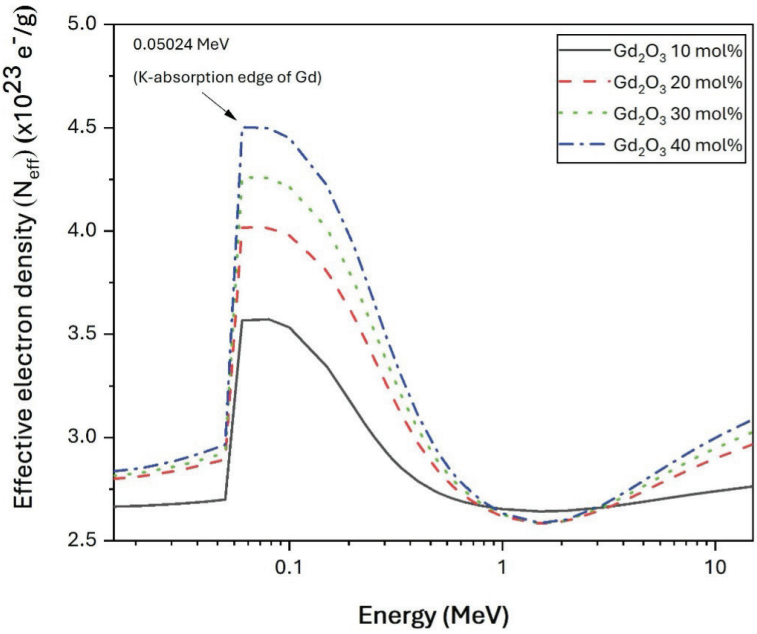

Figure 6. *The effective electron density of Gd_2O_3 added germanoborate glasses.*

Figure 7. illustrates the Half Value Layer (HVL) values of Gd_2O_3 added germanoborate glasses at a photon energy of 662 keV, as a function of Gd_2O_3 concentration (10-40 mol%). It is evident that HVL values decrease progressively with increasing Gd_2O_3 content, indicating enhanced gamma ray attenuation capability. This trend can be attributed to the high atomic number (Z = 64) of gadolinium, which significantly increases the probability of photon interactions particularly the photoelectric effect and Compton scattering within the glass matrix. For comparative, the HVL values of the Gd_2O_3 added glasses are plotted alongside standard shielding materials, including commercial window glass,[20] ordinary concrete,[21] and PbO Based Glass (50% PbO).[22] The results clearly demonstrate that all Gd_2O_3 added compositions possess superior shielding performance compared to both window glass and ordinary concrete. However, their HVL values remain higher than that of the PbO based glass, which is known for its excellent attenuation properties due to the high atomic number of lead (Z=82). Notably, the germanoborate glass sample containing 40 mol% Gd_2O_3 exhibits the lowest HVL among the studied compositions, highlighting its potential as a promising lead-free gamma ray shielding material.

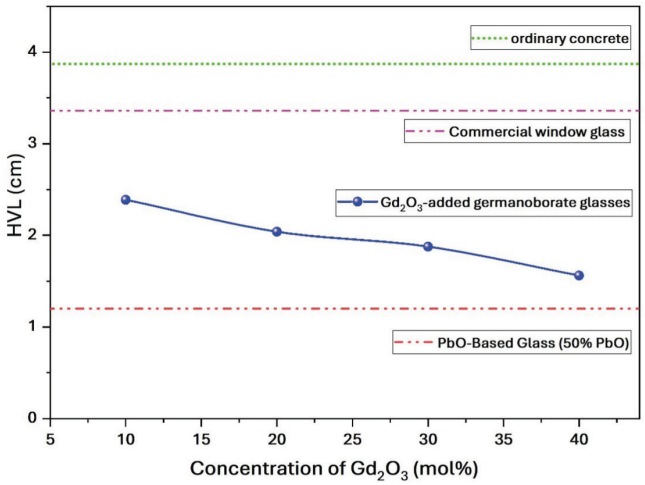

Figure 7. *The Half Value Layer (HVL) values of Gd_2O_3 added germanoborate glasses.*

The Pb equivalent of Gd_2O_3 added germanoborate glasses was determined for a thickness of 0.3 cm, as shown in Figure 8. From the results, the Pb equivalent of Gd_2O_3 added germanoborate glasses increases with the addition of Gd_2O_3. This trend indicates an enhancement in the materials radiation shielding capability, as higher Pb equivalent values correspond to greater attenuation effectiveness against ionizing radiation. When compared to standard reference shielding materials. The Pb equivalent values of the glasses are notably higher than those of commercial window glass,[21] but remain slightly lower than those of PbO-based glass compositions.[22]

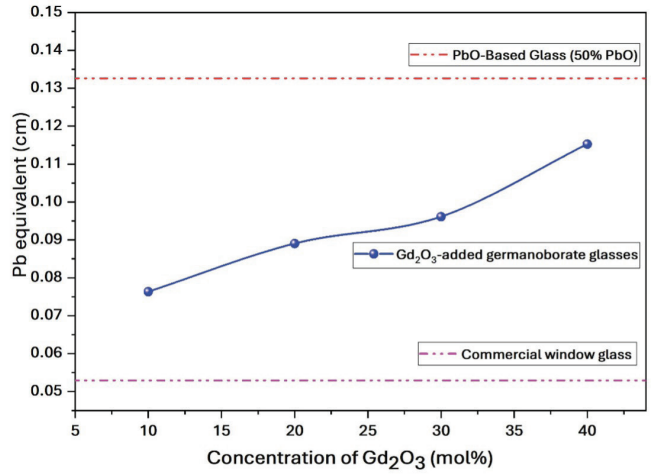

Figure 8. *The Pb equivalent of Gd_2O_3 added germanoborate glasses.*

The effective dose rate simulation

Figure 9 illustrates the effective dose rate (μSv/h) from gamma ray interactions with a computational phantom at an energy of 0.662 MeV. Simulations were performed using the PHITS software under anterior-posterior (AP) irradiation geometry to evaluate the shielding performance of Gd_2O_3 added glass at 40 mol%. The simulation results demonstrate a reduction in effective dose rate intensity when the Gd_2O_3 glass is used as a shielding material. Specifically, regions depicted in white, representing higher dose rates, are significantly diminished in the presence of 40 mol% Gd_2O_3 glass, while darker regions, indicating lower dose rates, become more prominent. This visual transition from white to deep blue or black suggests a decrease in gamma ray penetration, confirming the enhanced attenuation capability of the Gd_2O_3 glass. Figure 8(A) shows the effective dose rate distribution without any glass shielding material, with a maximum dose rate of 31.57 μSv/hr and a minimum of 0.1040 μSv/h. While Figure 8(B) which represents Gd_2O_3 glass at 40 mol%, shows a reduction in high dose regions, with dose rates ranging from 0.1315 μSv/hr (minimum) to 29.59 μSv/hr (maximum). These results highlight the effectiveness of Gd_2O_3 added glass in reducing radiation exposure in medical or shielding applications.

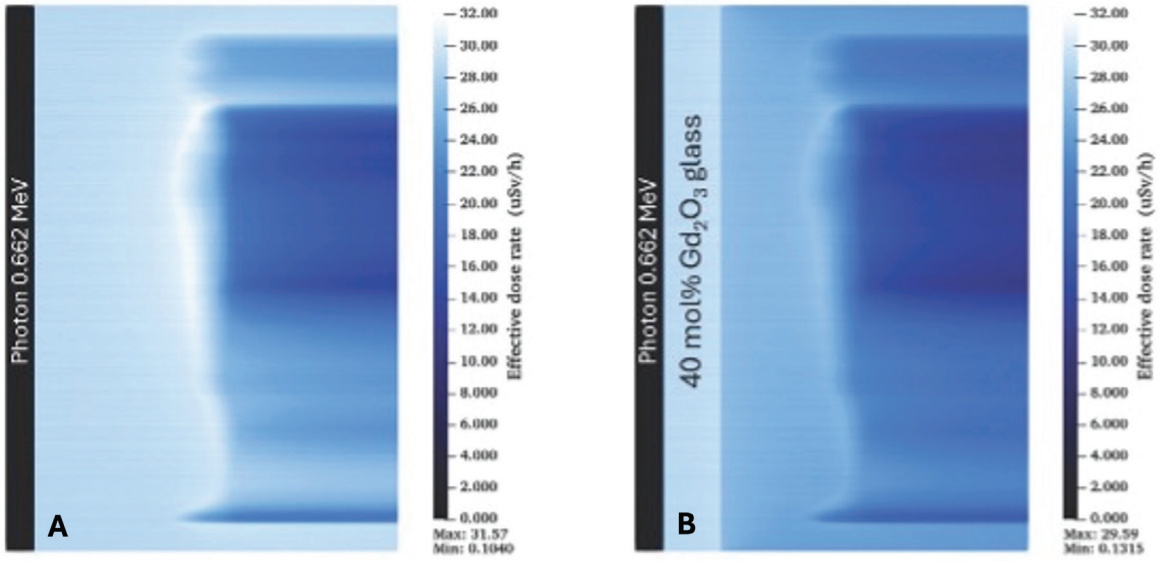

Figure 9. *The effective dose rate (μSv/h) simulation of glass in the energy range of 0.662 MeV. A: no glass, B: with Gd_2O_3 glasses at 40 mol%.*

Conclusion

In this work, the radiation shielding performance of Gd_2O_3 added germanoborate glasses with the composition (60-x)B_2O_3-GeO_2-Gd_2O_3 (x=10, 20, 30 and 40 mol%) was systematically investigated. The glasses were synthesized using the conventional melt quenching technique. Physical characterization revealed that increasing Gd_2O_3 content led to a rise in density from 3.7546 to 5.4604 gm/cm^3, while the molar volume initially increased. Radiation shielding parameters, including the mass attenuation coefficient (μ_m), effective atomic number (Zeff), and effective electron density (Neff), were evaluated over the energy range of 0.015-15 MeV using the WinXCom program. The results showed that all parameters followed the expected photon interaction mechanisms, which are dominated by the photoelectric effect at low energies, Compton scattering at intermediate energies, and pair production at high energies. Increasing the concentration of Gd_2O_3 resulted in higher values of these parameters, indicating improved radiation attenuation capability. From the HVL results, all Gd_2O_3 added germanoborate glasses exhibit superior shielding performance compared to commercial window glass and ordinary concrete, although their performance remains lower than that of PbO basedglass. Pb equivalent of glasses increases with Gd_2O_3 content, is significantly higher than that of commercial window glass, but remains slightly lower than PbO-based glass compositions. For the effective dose rate, the incorporation of 40 mol% Gd_2O_3 into the glass led to a noticeable reduction in high dose regions. These findings suggest that the incorporation of Gd_2O_3 significantly enhances the glass radiation shielding performance. Overall, the developed germanoborate glasses exhibit favorable physical and shielding properties, demonstrating strong potential for use as lead free transparent materials in radiation protection applications across medical, industrial, and nuclear fields.

Funding

National Research Council of Thailand for supporting this research (project number TSRI_68_3.3)

Conflict of interest

The authors declare no conflict of interest

CRediT authorship contribution statement

Natthakridta Chanthima: writing: original draft, validation, resources, investigation, funding acquisition, conceptualization; **Supakit Yonphan:** writing: review and editing, software, investigation; **Chalermpon Mutuwong**: methodology, investigation, software, conceptualization; **Wuttichai Chaiphaksa:** writing: review and editing, validation, conceptualization; **Jakrapong Kaewkhao:** writing: review and editing, supervision, conceptualization.

Acknowledgements

Authors would like to thank Thailand Science Research and Innovation (TSRI), Center of Excellence in Glass Technology and Materials Science (CEGM), Nakhon Pathom Rajabhat University and National Research Council of Thailand for supporting this research (project number TSRI_68_3.3)

References

[1] Safari A, Rafie P, Taeb S, Najafi M, Mortazavi SMJ. Development of lead-free materials for radiation shielding in medical settings: A review. JBPE. 2024; 14: 229-44. doi: 10.31661/jbpe.v0i0.2404-1742.

[2] Geist WH, Santi PA, Swinhoe Editors MT. Nondestructive assay of nuclear materials for safeguards and security.

[3] Bektasoglu M, Ali Mohammad M. Investigation of radiation shielding properties of TeO_2–ZnO–Nb_2O_5–Gd_2O_3 glasses at medical diagnostic energies. Ceram Int. 2020; 46(10): 16217-23. doi: 10.1016/j.ceramint.2020.03.177.

[4] Al-Buriahi MS, Kurtulus R, Eke C, Alomairy S, Olarinoye IO. An insight into advanced glass systems for radiation shielding applications: A review on different modifiers and heavy metal oxides-based glasses. Vol. 10, Heliyon. Elsevier Ltd. 2024; doi: 10.1016/j.heliyon.2024.e40249.

[5] Hordieiev Y, Zaichuk A. Structural, thermal, and radiation shielding properties of antimony-doped zinc borate glasses. Sci Rep. 2025; 15(1): 16158. doi: 10.1038/s41598-025-96015-5.

[6] Hongtong W, Kaewjaeng S, Kothan S, Meejitpaisan P, Cheewasukhanont W, Limkitjaroenporn P, et al. Development of gadolinium doped calcium phosphate oxyfluoride glasses for X-ray shielding materials. Vol. 5, Materials Today: Proceedings. 2018;https://doi.org/10.1016/j.matpr.2018.02.062

[7] Gerward L, Guilbert N, Jensen KB, Levring H. WinXCom - A program for calculating X-ray attenuation coefficients. In: Radiation Physics and Chemistry. 2004; pp 653-4. doi: 10.1016/j.radphyschem.2004.04.040.

[8] Özdoğan H, Üncü YA, Akman F, Polat H, Kaçal MR. Investigation of gamma ray shielding characteristics of binary composites containing polyester resin and lead oxide. Polymers (Basel). 2024; 16(23): 3324. doi: 10.3390/polym16233324.

[9] Elmahroug Y, Tellili B, Souga C. Determination of total mass attenuation coefficients, effective atomic numbers and electron densities for different shielding materials. Ann Nucl Energy. 2015; 75: 268-74. doi: 10.1016/j.anucene.2014.08.015.

[10] Shamshad L, Rooh G, Limkitjaroenporn P, Srisittipokakun N, Chaiphaksa W, Kim HJ, et al. A comparative study of gadolinium-based oxide and oxyfluoride glasses as low energy radiation shielding materials. Prog Nucl Energy. 2017; 97: 53-9. doi: 10.1016/j.pnucene.2016.12.014.

[11] Limkitjaroenporn P, Cheewasukhanont W, Kothan S, Kaewkhao J. Development of new high transparency Pb-free radiation shielding glass. Integr Ferroelectr. 2021; 214(1): 181-204. doi:10.1080/10584587.2020.1857196.

[12] Gerward L, Guilbert N, Bj(rn Jensen K, Levring H. X-ray absorption in matter. Reengineering XCOM [Internet]. Vol. 60, Radiat Phys Chem. 2001; doi:10.1016/S0969-806X(00)00324-8.

[13] Kim CH, Yeom YS, Petoussi-Henss N, Zankl M, Bolch WE, Lee C, et al. ICRP Publication 145: Adult mesh-type reference computational phantoms. Ann ICRP. 2020; 49(3): 13-201. doi: 10.1177/0146645319893605. PMID: 33231095.

[14] Petoussi-Henss N, Bolch WE, Eckerman KF, Endo A, Hertel N, Hunt J, et al. Conversion coefficients for radiological protection quantities for external radiation exposures. Ann ICRP. 2010; 40(2-5): 1-257. doi: 10.1016/j.icrp.2011.10.001.

[15] Sato T, Iwamoto Y, Hashimoto S, Ogawa T, Furuta T, Abe SI, et al. Recent improvements of the particle and heavy ion transport code system–PHITS version 3.33. J Nucl Sci Technol. 2024; 61(1): 127-35. doi: 10.1080/00223131.2023.2275736.

[16] Chaiphaksa W, Yonphan S, Mutuwong C, Kothan S, Intachai N, Kaewkhao J. Experimental, theoretical, and Monte Carlo simulation study of radiation shielding properties of La2O3-Added lithium borate glasses. Radiat Phys Chem. 2024; 224: 111994. doi: 10.1016/j.radphyschem.2024.111994.

[17] Madshal MA, El-Damrawi G, Abdelghany AM, Abdelghany MI. Structural studies and physical properties of Gd2O3-doped borate glass. J Mater Sc: Mater Electron. 2021; 32(11): 14642-53. doi: 10.1007/s10854-021-06022-1.

[18] Chandra SRM, Prabhakar RA, Krishnamurthy GK, Appa RB. Physical and optical properties of PbO-Sb2O3-B2O3 glasses doped with Gd2O3. In: Materials Today: Proceedings. Elsevier Ltd. 2016; pp 3970-5. doi: 10.1016/j.matpr.2016.11.058.

[19] Al-Buriahi MS, Alajerami YSM, Abouhaswa AS, Alalawi A, Nutaro T, Tonguc B. Effect of chromium oxide on the physical, optical, and radiation shielding properties of lead sodium borate glasses. J Non Cryst Solids. 20205; 544: 120171. doi: 10.1016/j.jnoncrysol.2020.120171.

[20] Madbouly AM, Alazab HA, Borham E, Ezz-ElDin FM.

Study of gamma radiation dosimeter and radiation shielding parameters of commercial window glass. Appl Phys A Mater Sci Process. 2021; 127(10): doi: 10.1007/s00339-021-04889-9.

[21] Singh K, Singh H, Sharma V, Nathuram R, Khanna A, Kumar R, et al. Gamma-ray attenuation coefficients in bismuth borate glasses. NIM-B. 2002; 194(10): 1-6. doi: 10.1016/S0168-583X(02)00498-6.

[22] Hussein EMA, Madbouly AM. Chemical and radiation shielding effectiveness of some heavy metal oxide glasses for immobilizing radioactive wastes. J Aust Ceram Soc. 2024; 60(1): 127-42. doi: 10.1007/s41779-023-00951-2.